

Article

# Cross-Layer Protocol Based on Directional Reception in Underwater Acoustic Wireless Sensor Networks

Yao Sun <sup>1,2,3</sup> , Wei Ge <sup>1,2,4,\*</sup>, Yingsong Li <sup>5</sup> and Jingwei Yin <sup>1,2,3</sup>

- <sup>1</sup> Acoustic Science and Technology Laboratory, Harbin Engineering University, Harbin 150001, China; sy6@hrbeu.edu.cn (Y.S.)
- <sup>2</sup> National Key Laboratory of Underwater Acoustic Technology, Harbin Engineering University, Ministry of Industry and Information Technology, Harbin 150001, China
- <sup>3</sup> College of Underwater Acoustic Engineering, Harbin Engineering University, Harbin 150001, China
- <sup>4</sup> Qingdao Innovation and Development Center, Harbin Engineering University, Qingdao 266000, China
- <sup>5</sup> College of Information and Communication Engineering, Harbin Engineering University, Harbin 150001, China
- \* Correspondence: gewei@hrbeu.edu.cn

**Abstract:** The long propagation delay of acoustic links leads to the complex randomness of packet collision, which reduces the network packet delivery rate (PDR) and aggravates network congestion. A single vector hydrophone with directional reception characteristics can concentrate the reception gain on a certain direction, which can increase spatial reuse, reduce packet collision, and help to improve the performance of the underwater acoustic wireless sensor networks (UASNs). Herein, this paper proposes a cross-layer protocol with low interference and low congestion (CLIC) based on directional reception. An integrated routing-medium access control (MAC) design is also devised in the CLIC scheme to use the directional beams to create the least-interfering, highest-capacity data transmission links, weighing key factors affecting network performance to obtain routes with low collisions and low congestion. Simulation results show that the CLIC has a higher packet delivery rate (PDR) and higher energy efficiency compared to the QELAR, CITP, and VBF protocols.

**Keywords:** underwater acoustic sensor networks; routing; directional reception



**Citation:** Sun, Y.; Ge, W.; Li, Y.; Yin, J. Cross-Layer Protocol Based on Directional Reception in Underwater Acoustic Wireless Sensor Networks. *Mar. Sci. Eng.* **2023**, *11*, 666. <https://doi.org/10.3390/jmse11030666>

Academic Editor: Rafael Morales

Received: 22 February 2023

Revised: 11 March 2023

Accepted: 19 March 2023

Published: 21 March 2023



**Copyright:** © 2023 by the authors. Licensee MDPI, Basel, Switzerland. This article is an open access article distributed under the terms and conditions of the Creative Commons Attribution (CC BY) license (<https://creativecommons.org/licenses/by/4.0/>).

## 1. Introduction

The long propagation delay and low transmission rate of underwater acoustic communications and the dynamic marine communication environment pose serious challenges in designing underwater acoustic wireless sensor networks (UASNs) protocols [1–4]. For an omnidirectional underwater acoustic communication network scenario, nodes use omnidirectional transmission to send and receive packets. Due to the nature of broadcasting, the network performance is seriously affected by the large propagation delay and high packet collision rate [5–7]. Although the handshake mechanism of the competitive MAC protocol widely used in UASNs can reduce the occurrence of collision, there are still problems of wasting idle channels and low spatial reuse [8]. The MAC protocol in [7] uses a handshake to compete for channels, reducing network collisions, but it still suffers from low spatial reuse. Development of underwater acoustic directional communication technology has been paid more attention with the increasing interest in applying directional reception technology to UASNs to improve network performance. Different from omnidirectional transceiver networks, the sound pressure and vibration velocity of the acoustic vector sensors form unilateral directivity through linear weighting combination to achieve directional reception of signals in a certain direction, thereby improving the spatial reuse rate of the network.

Although the application of vector hydrophone in wireless networks has been widely studied, the research in UASNs is relatively limited, which is mainly limited by the media

access control protocol and channel difference. Some studies of UASNs routing and MAC schemes using directional transmission are reported in [9,10].

Liu et al. proposed a directional MAC framework based on the vector hydrophone and multimodal transducer, along with a benchmark MAC protocol, which can achieve spatial reuse and energy conservation [9]. Simulation results show that the MAC protocol outperforms existing representative protocols in terms of throughput, end-to-end delay, and energy efficiency. Yang et al. introduced the validity of conventional routing schemes in underwater ad hoc networks with directional antennas and presented a special design of multipath routing algorithm for directional transmission. The experimental results show a significant performance improvement in throughput and latency [10].

Although there are many routing or MAC protocols based on directional transmission, most do not take into account the collision-prone and congestion-prone nature of packets in hydroacoustic networks.

The node deployment of the UASNs is sparse, so it is easy to cause network congestion under heavy and burst data input loads such as earthquake monitoring applications. Network congestion always leads to packet loss, packet interference, and queuing delays, which degrades network performance [11]. As we know, more interference increases packet collisions and reduces the packet delivery rate (PDR). Although directional reception techniques obtain higher network capacity, the long propagation delays of acoustic links still lead to packet collisions. Therefore, interference avoidance and congestion control are critical for the UASNs to achieve high throughput and long network lifetime. This paper describes a cross-layer protocol with low interference and low congestion (CLIC) based on directional reception. An integrated routing-MAC is employed in the CLIC to use directional beams to create the least-interfering, highest-capacity data transmission links, weighing key factors affecting network performance to obtain routes with low collisions and low congestion. Simulation results show that the CLIC has a better PDR and higher energy efficiency compared to the machine-learning based adaptive routing protocol (QELAR) [12] and vector-based forwarding (VBF) [13] protocols.

The main contributions of this paper are presented as follows:

1. Based on the fact that the relays face higher packet collisions with more interfering neighbors, a relay selection scheme based on neighbor interference and congestion level is proposed, which provides high PDR and low latency routes with lower overhead by weighing the key factors affecting network performance.
2. A MAC protocol with a channel reservation mechanism is also presented. Nodes compete for channels by Contend packets (CT). The degree-of-congestion in the transmitting node and the degree of interference in the receiving node determine the priority of the CT. According to the characteristics of single vector hydrophone directional reception, the backoff of nodes depends on the degree of interference caused by data transmission, which reduces network congestion and packet collisions and improves bandwidth and energy efficiency.
3. The CLIC with a directional reception mode is proposed on the basis of the spatial multiplexing property of directional reception using vector hydrophones. In addition, an integrated routing-MAC is used in a route to adaptively bypass nodes with high collision probability and high congestion level.

The remainder of this paper is organized as follows: In Section 2, we review the related literature. The network model is presented in Section 3. Section 4 describes the proposed DM protocol, and its performance evaluation is presented in Section 5 via comparative simulations. Section 6 is a short conclusion.

## 2. Related Work

Many different routing schemes have been presented and used for the UASNs due to the unique characteristics of underwater acoustic channels, including long propagation delays, low data rate, and high error probability.

Vector-based forwarding (VBF) is a geographical location routing method [13] that limits the forwarding range of data packets to the virtual pipeline determined by the source node and the destination node. An effective anycast routing algorithm called HydroCast [14] uses a new opportunistic routing mechanism to select a subset of forwarders that maximizes greedy processes but limits interference on the same channel and employs an efficient method for recovering underwater dead zones. HydroCast has achieved superior performance to both depth-based routing (DBR) [15] and an efficient 3D cube-based protocol [16].

An RL-based routing protocol for UASNs named QELAR has been proposed [12]. In QELAR, the reward function is composed of the residual energy of the nodes and the energy distribution among a group of nodes, and the network life is extended by balancing the residual energy. Simulation results show that the average service life of QELAR is 20% longer than that of VBF [13]. A congestion avoidance routing protocol for UASNs based on RL has been developed [17] in which the reward function is defined by the current buffer state, residual energy, and location information of the neighbors. To accelerate the convergence of the algorithm, a dynamic virtual routing pipeline with a variable radius is introduced, which is related to the average residual energy of the sender node's neighbors. A localization-free interference and energy holes minimization (LF-IEHM) routing protocol for UASNs has been proposed [18]. The proposed algorithm overcomes interference during data packet forwarding by defining a unique packet holding time for every sensor node. The energy holes formation is mitigated by a variable transmission range of the sensor nodes.

Cross-layer design, where more than one layer in the protocol stack interacts with each other, has been drawing the attention of researchers over the past few years as a promising performance management technology in UASNs with complex channels.

Shashaj et al. [19] followed a cross-layering design and provided a class of scheduling, power control, and routing policies that result in low-power, interference-aware effective solutions for underwater sensor networks. Considering the complete interference model, they assumed the accurate description of an underwater acoustic channel and modeled the acoustic signal attenuation and propagation through Bellhop ray tracing software.

Inspired by the unpredictability of both route interruptions and packet collisions in UASNs, a collision and interruption tolerant protocol (CITP) was proposed to jointly address the two challenges in a smart way [20]. By exploiting the opportunistic transmission strategy, CITP forms the optimized route on the fly, which bypasses nodes that undergo collisions or interrupted links and void regions. An energy-efficient, channel-aware, and depth-based scalable and multipath-agent-based routing protocol (ABA) is proposed in [21]. ABA considers multiple parameters, such as node energy, propagation delay, link quality, hop count, and queue size to select the relay node. ABA adopts a cross-layer approach to estimate the quality of link that assures higher reliability than the probabilistic measure. The propagation time is also taken into account with varying depth, temperature, and salinity. The propagation time and quality of link are vital factors that ensure the speed of data transmission and reliability.

### 3. System Model

#### 3.1. Vector Hydrophone

Assume that in the initial state,  $n$  sensor nodes are randomly and non-uniformly distributed in the three-dimensional underwater area to collect the underwater environment information and send data to a sink node on the sea surface, where each node is equipped with a vector hydrophone. The receiving mode is directional reception, and the transmitting mode is omnidirectional transmission. The vector hydrophone is a composite of a conventional non-directional-type acoustic pressure hydrophone and a plasmonic vibration hydrophone [22,23], which can simultaneously measure the orthogonal components of acoustic pressure and plasmonic vibration velocity. Therefore, compared to the acoustic pressure hydrophone, the vector hydrophone has more output signals that consist of acoustic pressure signal  $p(t)$  and two vibration velocity signals  $v_x(t)$ ,  $v_y(t)$ , which is expressed as

$$\begin{cases} p(t) = x(t) \\ v_x(t) = x(t) \cos \theta \cos \psi \\ v_y(t) = x(t) \sin \theta \cos \psi \end{cases} \quad (1)$$

where  $\theta$  is the horizontal azimuth angle, and  $\psi$  is the pitch angle of the incident acoustic wave.

The directional of the vibration speed sensor can be electronically rotated, and we define  $v_c(t)$  and  $v_s(t)$  as the combined directional after electronic rotation, and

$$\begin{cases} v_c(t) = v_x(t) \cos \varphi + v_y(t) \sin \varphi = x(t) \cos(\theta - \varphi) \\ v_s(t) = v_x(t) \sin \varphi + v_y(t) \cos \varphi = x(t) \sin(\theta - \varphi) \end{cases} \quad (2)$$

where  $\varphi$  is the guiding direction. A linear combination of  $p(t)$  and  $v_c(t)$  is usually used in hydro-acoustic communication to improve the signal-to-noise ratio (SNR) of the received signal. In this paper, we use  $p + 2 \cdot v_c$ .

### 3.2. Communication Model

In an omnidirectional network, nodes adopt omnidirectional transmission and omnidirectional reception (OO) communication mode. In this mode, packets will be heard by all nodes within communication range. Its advantage is that communication nodes are easier to coordinate, but its disadvantage is that it is easy to cause packet collisions and waste channel capacity. Vector hydrophones have been widely used in hydroacoustic sensor networks due to their ability to increase the spatial reuse rate of the network. In this paper, an omnidirectional transmit and directional receive (OD) communication mode is used. In the OD communication mode, packets can only be received by nodes whose beams are facing the sending node. This mode reduces communication interference between nodes, but in order to increase network throughput, reservation coordination between nodes is also required. The comparison of the two communication modes is shown in Figures 1 and 2.

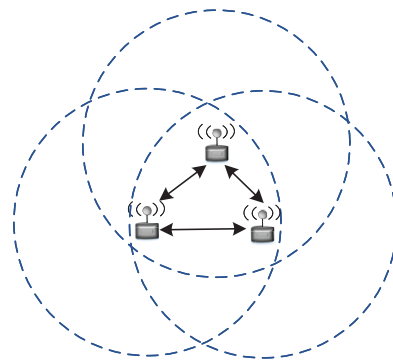


Figure 1. Communication mode of OO.

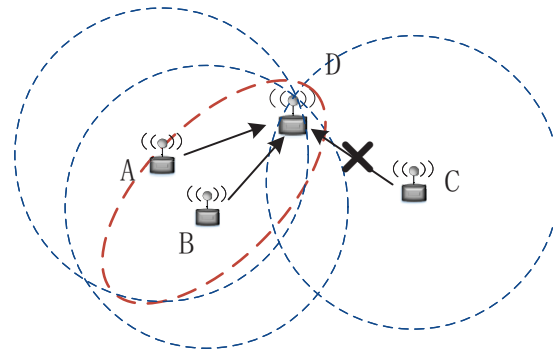


Figure 2. Communication mode of OD.

Figure 1 is a visualization of the OO communication mode, where packets are received by all nodes in communication range. Figure 2 is a visualization of the OD communication mode. Nodes A and B are within the beam of node D, and node C is not, so packets sent by nodes A and B can be received by node D, while packets sent by node C cannot be received by node D.

Assume that there is a pair of transmitter  $T_0$  and receiver  $R$  and that there are  $K$  interfering  $T_i$  ( $i = 1, 2, \dots, M$ ) at  $R$ .

In the OO mode, ignoring the influence of noise, the received signal can be expressed as:

$$y(t, f) = \sum_{i=0}^M H_i(d_i, f) \text{Re}\{s(t)e^{j2\pi ft}\}, \tag{3}$$

where  $f$  is the communication carrier frequency, and  $d_i$  is the distance from  $T_i$  to  $R$ ,  $H_i(d_i, f)$  is the channel gain of the  $T_i$  signal reaching  $R$ , and  $x_i$  denotes the signal sent by  $T_i$ .

Assuming that the angle between the interferer  $T_i$  and the receiver  $R$  receives the pointing direction  $\theta_i$ , and that the pointing reception uses  $p + 2 \cdot v_c$  of the vector combination mode, then the output of the signal sent by  $T_i$  at  $R$  is:

$$y_i(t, f) = H_i(d_i, f) \text{Re}\{s(t)e^{j2\pi ft}\} [1 + 2 \cos(\theta_i)] \tag{4}$$

If the distance from  $T_i$  to the receiver is  $d_i$  and the center frequency is  $f$ , the channel gain  $H_i(d, f)$  at the receiver of the underwater acoustic signal sent by  $T_i$  follows the complex Gaussian distribution, and the variance of this distribution is:

$$\sigma_i^2(d_i, f) = d_i^{-k} k(f)^{-d_i}, \tag{5}$$

where  $k$  is the propagation coefficient related to the marine geographical environment ( $k$  is usually taken as 1.5), and  $k(f)^{-d_i}$  is the absorption coefficient related to distance  $d_i$  and frequency  $f$ .

The signal-to-interference noise ratio (SINR) model at  $R$  is expressed as:

$$\text{SINR} = \frac{P_t \cdot (H_i(d_i, f))^2 \cdot G(0)}{\sum_{j=1}^M P_t \cdot (H_j(d_j, f))^2 \cdot G(\theta_j) + P_n}, \tag{6}$$

where  $P_t$  is the transmission power of  $T_i$ , and  $P_n$  is the noise power at  $R$ . Assuming that the sound pressure noise power is  $\sigma_n^2$ , the vibration speed noise power is  $\frac{\sigma_n^2}{2}$ , and the noise power is  $3\sigma_n^2$  in the linear combination  $p + 2 \cdot v_c$ , so the values of  $P_n$  under omnidirectional and directional reception models are  $\sigma_n^2$  and  $3\sigma_n^2$ , respectively.  $\theta_j$  denotes the angle between the orientation of  $T_j$  to  $R$  and the  $R$  extreme pointing orientation.

#### 4. Proposed CLIC Protocol

Assume that the nodes know their location and the location of the sink node. Localization algorithms [24,25] can be used to obtain these geographic coordinates. Using the vector hydrophone localization algorithm, nodes can determine the relative positions of neighboring nodes [26].

Based on the routing algorithms and MAC designs for interference and congestion avoidance, the CLIC forms a route that adaptively bypasses nodes with high packet collision probability and high congestion, reducing duplicate packet forwarding and end-to-end delay.

##### 4.1. Low-Complexity Routing Protocols for Interference and Congestion Avoidance

Interference and congestion avoidance are critical for networks to achieve high throughput and long lifetime. In particular, it is important that routing protocols provide low interference and congestion paths in the context of achieving metrics, such as throughput,

latency, and packet delivery rates. To avoid interference and congestion, routes need to bypass interference and congestion areas in order for packets to reach the sink reliably and quickly.

In the CLIC, the routing protocol consists of three main phases: the initialization phase, the relay selection phase, and the packet forwarding phase.

During the initialization phase, nodes obtain their remaining energy and location information from the physical layer. Then, the information, such as the current buffer state and the number of interfering nodes in the neighbourhood, is exchanged via broadcast packets. Each node generates a neighbor table during the initialization phase to store each neighbor's information for routing decisions.

In the relay selection phase, the node selects a relay based on the information in the neighbor table, combining with metrics, such as throughput, delay, packet loss rate, and lifetime. The node first calculates the priority of the neighbor nodes and selects the node with the highest priority as the relay. The priority of neighbor node  $j$  of node  $i$  is given

$$P_j = \alpha \times Energy(j) + \beta \times Hops(j) + \gamma \times Cong(j) + \lambda \times Interf(j), \quad (7)$$

where  $\alpha$ ,  $\beta$ ,  $\gamma$ , and  $\lambda$  are the coefficients for energy, delay, congestion, and interference, respectively.

$$Energy(j) = \begin{cases} 1, & x > 0 \\ e^x, & x < 0 \end{cases} \quad (8)$$

$$x = E_{res}(j) - \bar{E}_{res}(j) \quad (9)$$

$Energy(j)$  represents the relationship between the residual energy of node  $j$  and the average residual energy of its neighbor nodes,  $E_{res}(j)$  is the residual energy of node  $j$ , and  $\bar{E}_{res}(j)$  is the average residual energy of the neighbor nodes of  $j$ . When the residual energy of node  $j$  is greater than the average residual energy of neighbor nodes,  $Energy(j) = 1$ ; otherwise, it is a real number between 0 and 1.

Extending network lifetime is a necessary goal to be considered for routing protocol developments. If a node is often selected as a relay, it becomes a hotspot and will die prematurely due to its frequent involvement in data transmission. The energy factor of the nodes is incorporated into priority evaluation, and the nodes with higher residual energy are preferred to be selected as relays, thus avoiding a hotspot problem.

$Hops(j)$  is the estimated number of hops from node  $i$  to sink when node  $j$  is selected as a relay;  $d_{i-sink}$  is the distance between node  $j$  and sink, and  $\langle d_{ij} \rangle_{i-sink}$  is the projection of  $d_{ij}$  onto the line connecting node  $i$  with the sink.

Closer to the sink has higher priority, which reduces the detour path and decreases the end-to-end delay. Although it is easy to estimate the number of distant links, this method does not incur any signaling overhead because it is computed locally and does not require end-to-end information exchange, which is suitable for the UASNs with unstable links to save energy.

$$H_{ij}^{hops} = \max\left(\frac{d_{i-sink}}{\langle d_{ij} \rangle_{i-sink}}, 1\right), \quad (10)$$

$Cong(j)$  is the congestion factor considered in relay selection.  $Buff_{now}$  is the current buffer length of the neighboring node, and  $Buff_{max}$  is the maximum buffer length of the node.

$$Cong(j) = 1 - \frac{Buff_{now}}{Buff_{max}} \quad (11)$$

Nodes with less data in the buffer have lower congestion. There is a preference to select nodes with lower congestion as relays to avoid high congestion areas.

$Interf(j)$  is the interference factor taken into consideration in relay selection.  $Nei_j$  is the set of neighbouring nodes at node  $j$ .  $Interf_j^i$  is the set of nodes that may cause interference to node  $j$  when receiving packets sent by node  $i$ .

$$Interf(j) = 1 - \frac{|Inter_j^i|}{|Nei_j|}, \tag{12}$$

$$Nei_j = \{j' | d(j, j') < range\}, \tag{13}$$

$$Inter_j^i = \{j' | SNR_{j'} = SL - TL_{j'} - NL_{j'} + G_{j'} \geq DT\}, \tag{14}$$

where  $SNR_{j'}$  is the received signal-to-noise ratio of the signal sent by node  $j'$  at node  $j$ , and  $DT$  is defined as the detection threshold.  $SL$  is the target source level,  $TL_{j'}$  is transmission loss due to water environment,  $NL_{j'}$  is the noise level (from the receiver + the environment), and  $G_{j'}dn$  is combined gain of the vector hydrophone.

The spatial and temporal uncertainty of the underwater acoustic channel leads to a high packet collision probability. Information interaction allows a sending node to know how many nodes in the vicinity of the receiving node may cause interference to a transmission, thus actively avoiding high interference areas and reducing packet collisions. The directional reception technique also reduces the interference range so that the number of interfering nodes is less than or equal to the total number of neighbors.

When nodes are to forward packets, the forwarding priority of each neighbor is calculated based on the information in the neighbor table. The evaluation of priority incorporates energy, distance advance, interference, and congestion, where the relay selection is shown in Figure 3. Node 1 transmits packets to the sink node, and Nodes 2, 3, and 4 are candidate relay nodes. Node 4 has more interfering neighbour nodes and does not have a distance advantage, so it has low priority. Node 3 has a similar distance advantage to Node 2, but Node 2 has fewer packets in its buffer, so it has a higher priority than Node 3. Node 1 will choose Node 2 as the best relay. Interference and congestion avoidance is achieved by avoiding high interference and high congestion areas. In summary, the proposed routing solution allows node  $i$  to select node  $j$  as a relay that satisfies the following rules: (1) it is closer to sink than  $i$ , (2) it has higher energy, (3) it has lower transmission interference to  $i$ , and (4) it has a shorter buffer queue (low congestion).

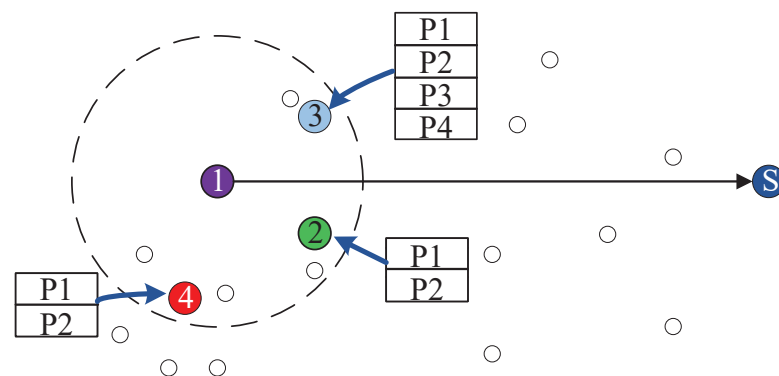


Figure 3. Relay selection scheme.

#### 4.2. Collision-Tolerant MAC Protocol with CT Priority

A single vector hydrophone with directional reception characteristics can concentrate the reception gain on one direction, which can reduce energy loss and increase spatial reuse. Therefore, for directional reception mode, if the MAC protocol of the omnidirectional reception mode is also used, it will cause channel waste. Thus, a contention-based collision-tolerant MAC protocol (DMAC) is presented based on directional reception. The DMAC combines time slot and channel contention mechanisms to provide a MAC protocol with efficient channel utilization, low interference, and low latency. The DMAC defines three types of packets: CT, data packet (DATA), and acknowledge (ACK). To keep the neighbor table up to date, all three packets contain node information within them.

To avoid packet collision, each packet must be transmitted at the beginning of the time slot. The length of the time slot is

$$slot = \tau + T_{trans} + T_{guard}, \tag{15}$$

$$\tau = \frac{range}{v}, \tag{16}$$

where  $\tau$  is the maximum propagation delay, and  $T_{trans}$  is the packet transmission delay. Different packets have different transmission delays.  $T_{guard}$  is the guard time slot, which is 0.0001 s.

The design for the directional receive handshake mechanism in this paper is presented as

1. When a node aims to send a packet, it waits until the slot start and competes for a channel by sending a CT packet that includes the next-hop address determined by the relay selection algorithm, its own remaining energy, buffer queue length, number of potential interferences, and the priority of the contention channel. After receiving the CT, the node first updates the neighbor information table and then determines the next slot action based on the CT that is given by

$$P = \zeta \cdot \left(1 - \frac{|Inter_j^i|}{|Nei_j|}\right) + \delta \cdot \left(1 - \frac{Buf f_{now}}{Buf f_{max}}\right), \tag{17}$$

where  $\zeta$  and  $\delta$  are the weights of interference and congestion, respectively. If the node has a low level of congestion and the packet transmission has a low potential interference, the CT has a high priority and is more likely to compete for channel success. The priority is designed to make the network less congested, balance the traffic, and reduce packet interference.

2. After receiving a CT packet intended for another node (xCT), it does not need to enter into silent state immediately but makes a judgment based on the interference situation.
  - A node that has sent a CT first compares the priority of two CT packets. If its own CT packet priority is lower than that of the xCT, it will determine whether its next data transmission will interfere with the data transmission of the node with the higher priority. If the interference power is greater than the acceptable average interference power threshold ( $MeanP$ ), it is silent long enough for the node with high priority to transmit the DATA and ACK.
  - If the interference power is less than the  $MeanP$ , then it determines whether the transmission with higher priority will interfere with its own data transmission. If they do not interfere with each other, the node does not silence, keeping its current state and sending DATA for the next slot. The  $MeanP$  is defined as

$$MeanP = \frac{S_{th} - SINR}{|Inter_j^i|}, \tag{18}$$

where  $S_{th}$  is the received power, and SINR is the received power threshold.

- Nodes that do not send CT packets silence two time slots (DATA and ACK) to allow another terminal to transmit DATA and receive the corresponding ACK. If a DATA packet sent to itself is received during silence, it determines whether sending an ACK in the next slot will affect the receiving ACK of the node with high priority. If there is no effect (interference power is less than  $MeanP$ ), an ACK is sent in the next slot after receiving the DATA. Otherwise, it will remain silent.

The interference determination scheme is given in Figure 4. As shown in Figure 4, Nodes 1, 2, 3, and 6 have sent CT packets, and Node 1 has the highest priority. Since the interference power of packets sent from Node 2 and received by Node R is greater

than MeanP, Node 2 is silent. The interference power of the packets received by Node R from Node 3 and Node 6 is less than MeanP. When Node 6 transmits data to Node 7, since Node 7 is outside the transmission range of Node 1, the packet transmission of Node 1 will not affect the packet reception of Node 7, so Node 6 can transmit packets in the next slot. When Node 3 transmits data to Node 4, Node 4 is located within the transmission range of Node 1, so Node 3 cannot transmit data to Node 4, and Node 3 remains silent.

3. After the CT slot, the nodes that are not silent will transmit the DATA and wait for the ACK in the next slot.

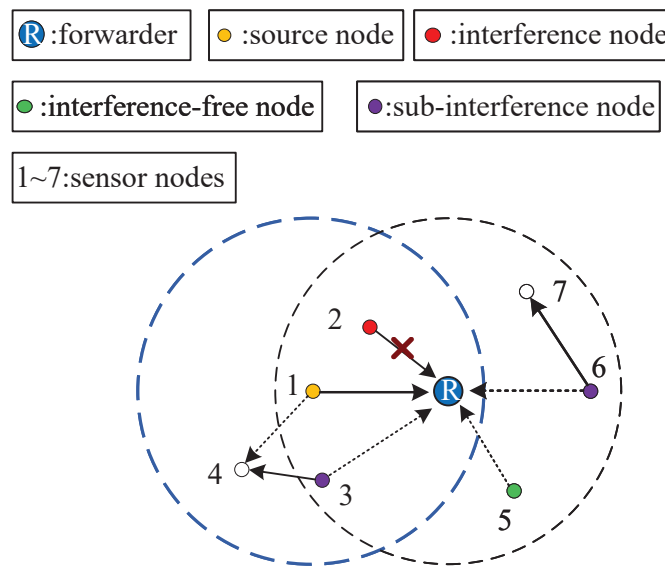


Figure 4. Interference determination scheme for DMAC.

Figure 5 is an overview of DMAC. At the beginning of the CT slot, nodes send CT contention channels. Nodes with high CT priority send packets in the next slot and wait for ACK in the ACK slot.

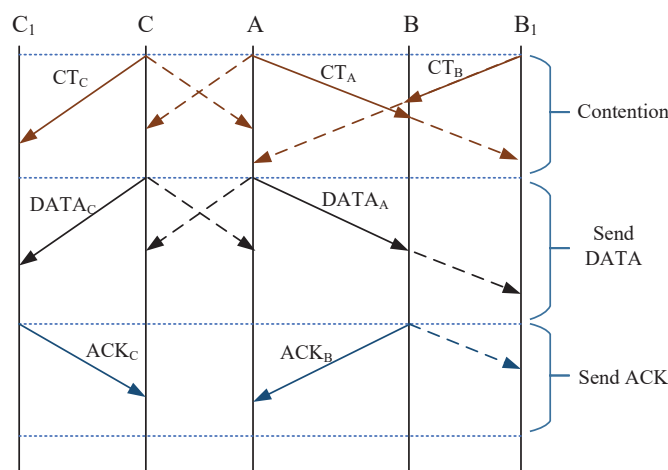


Figure 5. Overview of DMAC.

#### 4.3. Overview of CLIC

The process of the CLIC protocol is described in Algorithm 1. From Algorithm 1, the main steps of the CLIC algorithm are as follows.

Step 1: Initialize the parameters, e.g.,  $Buf_{max}$ ,  $range$ , initial energy, and coordinates of nodes.

- Step 2: Broadcast a beacon to obtain neighbor information., e.g.,  $Buf_{f_{now}}$ ,  $Nei$ ,  $MeanP$  and coordinates.
- Step 3: Calculate the priority of the neighbor using (7).
- Step 4: Select the highest priority neighbor as relay.
- Step 5: Calculate the priority of CT using (17).
- Step 6: Send CT at the beginning of the CT slot.
- Step 7: If xCT is received, update the neighbor information.
- Step 8: Compare the priority of CT and xCT.
- Step 9: The nodes with high CT priority send DATA at the beginning of the DATA slot.
- Step 10: Nodes with low CT priority determine whether their own data transmissions and those with high CT priority interfere with each other.
- Step 11: Back off if it interferes with data transmission.
- Step 12: Send DATA if it does not interfere with data transmission at the beginning of the DATA slot.

---

#### Algorithm 1 CLIC Algorithm

---

```

1: Initialize network;
2: Broadcast beacon;
3: Get  $E_{res}$ ,  $Buf_{f_{now}}$ ,  $Buf_{f_{max}}$ ,  $Inter$ ,  $MeanP$  and location of Neighbor;
4: Begin
5:   // Before sending data
6:    $calPriority()$ ;
7:    $getRelay()$ ; //Obtain the best relay using (7)
8:    $calPriCT()$ ; //Obtain CT priority using (17)
9:    $sendCT()$ ; //At the beginning of CT slot
10:  If received xCT then
11:     $updateNei()$ ;
12:     $compareCT()$ ;
13:    If ( $p_{CT} \geq p_{xCT}$ ) then
14:       $sendData()$ ; //At the beginning of DATA slot
15:    Else If (no interference with each other) then
16:       $sendData()$ ;
17:    Else
18:       $backoff()$ ;
19:    End If
20:  End If
21: End

```

---

It can be seen from (7) that a node can maximize priority, which will be chosen as the best relay, meaning that the node does not need to solve a complex optimization problem to find the global optimal path. On the contrary, it sequentially finds the local optimal solution. Therefore, the CLIC has low complexity, which is proportional to the number of the neighbor nodes.

## 5. Simulation Results

In this section, we evaluate the performance of the CLIC for UASNs using the NS3 platform. First, simulation settings are given to analyze how relevant parameters affect network performance. The performance of different routing protocols is then compared in terms of PDR, end-to-end delay, energy consumption, and energy efficiency. The PDR is the ratio of the number of packets successfully received by the sink to the number of packets sent by source nodes. End-to-end delay is the routing time of data packets transmitted from source nodes to the sink. Energy efficiency is defined as the ratio of the total size of successfully received data packets to the total energy consumed by the network. The common parameters used in the simulation are presented in Table 1.

**Table 1.** System symbols.

Parameter	Value
Number of sensor nodes	55~75
Simulation area	3 km × 3 km × 1 km
Transmission range	1 km
Initial energy	30,000 J
Transmission power	8 W
Receiving power	0.8 W
Idle power	20 mW
Data packet size	256 bytes
Packet generation rate	0.001 (packets/s)~0.0055 (packets/s)
Transmission rate	2000 bps
Simulation time	20,000 s

A UASN consisting of multiple sensor nodes and a sink node is considered. Sensor nodes are evenly and randomly distributed in a three-dimensional space measuring 3 km × 3 km × 1 km and are allowed to move randomly with a maximum speed of 1 m/s. They continuously send data packets to the sink through multi-hop routing. The sink node is fixed on the surface of the network and has infinite energy.

5.1. Performance Evaluation of CLIC

The CLIC protocol focuses on low interference and congestion. From (7), we know that  $(\alpha, \beta, \gamma, \lambda)$  has important effects on the CLIC, which needs to be well investigated. Here, effects of  $(\alpha, \beta, \gamma, \lambda)$  on energy consumption, end-to-end delay, congestion, and interference are investigated with settings of  $(\frac{1}{4}, \frac{1}{4}, \frac{1}{4}, \frac{1}{4})$ ,  $(\frac{3}{4}, \frac{1}{4}, 0, 0)$ ,  $(0, 1, 0, 0)$ ,  $(0, \frac{1}{4}, \frac{3}{4}, 0)$ , and  $(0, \frac{1}{4}, 0, \frac{3}{4})$ , respectively.

Figure 6 shows the end-to-end delay of CLIC under different parameters. It can be seen that the end-to-end delay of the network is mainly affected by network congestion and collision. The effect of distance on the end-to-end delay is enhanced when there are a sufficient number of nodes in the network. The emphasis on energy in relay selection is not conducive to reducing end-to-end delay.

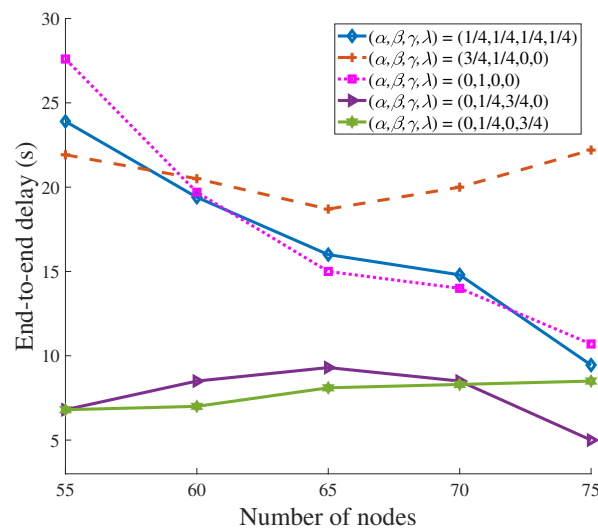


**Figure 6.** End-to-end delay of CLIC.

From Figure 7, it can be found that the highest PDR can be obtained when energy, distance, congestion, and interference factors are also considered in relay selection. The network also achieves a high PDR when only the distance factor is considered because packets are always delivered in the direction of the sink, reducing detours and decreasing packet

transmission failure probability. The network also achieves a high PDR when the weight of the interference factor is increased.

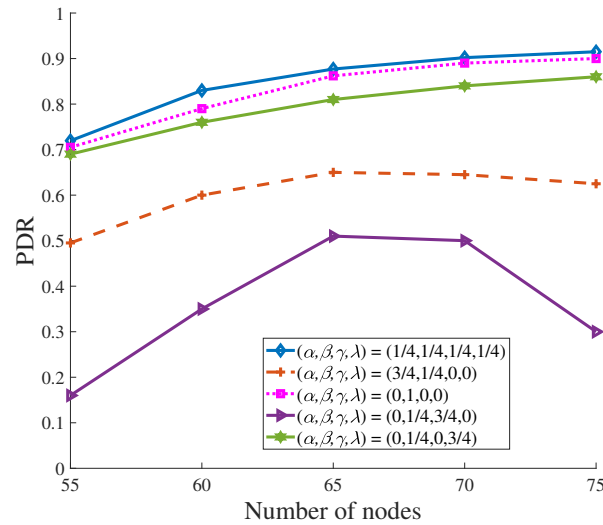


Figure 7. PDR of CLIC.

As shown in Figure 8, relay selection that considers all four factors together achieves better energy efficiency. Lower energy consumption can also be achieved if the focus is only on distance advancement. Relay selection that considers energy, congestion, and interference factors alone does not achieve high energy efficiency as it leads to detour routes.

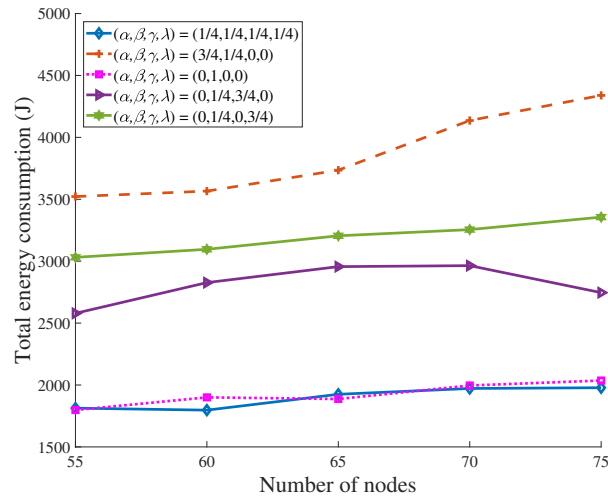


Figure 8. Energy consumption of CLIC.

A relatively balanced weight distribution is conducive to ensuring the stability of the network. According to the above simulation analysis, we set  $(\alpha, \beta, \gamma, \lambda) = (\frac{1}{4}, \frac{1}{4}, \frac{1}{4}, \frac{1}{4})$  to obtain optimal network performance.

### 5.2. Performance Comparisons

In this section, the performance of CLIC is compared with that of the RL-based QELAR [12], the geolocation-based VBF [13] with different pipelines of 600 m and cross-layer protocol CITP [20] with a focus on interference and collisions. Meanwhile, we analyze the influence of the weight values ( $\zeta$  and  $\delta$ ) on the performance of CLIC, as the priority of CT is influenced by the weights  $\zeta$  and  $\delta$ . All protocols are compared in the same three-dimensional space.

Figure 9 shows the relationship between the end-to-end delay of different protocols and the number of nodes. From Figure 9, it can be seen that the end-to-end delay of CLIC is not much higher than that of the VBF but much less than that of the QELAR, and it decreases as the number of nodes increases because the relay selection of the CLIC takes into account the important factors (end-to-end distance, node congestion, and interference) that affect the end-to-end delay as well as the reduced handshake MAC protocol that reduces end-to-end delay.

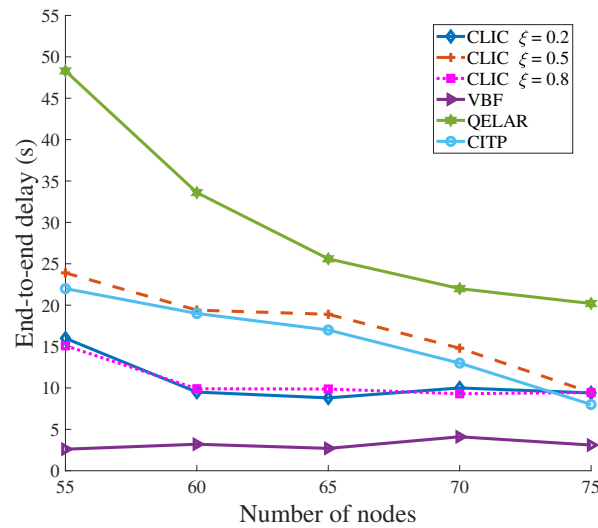


Figure 9. Comparison of end-to-end delay versus the number of nodes.

Figure 10 demonstrates the packet delivery ratio of different protocols with different numbers of nodes. Due to the integrated routing-MAC, the CLIC obtains a higher PDR than those of the QELAR and VBF and is stable as the number of nodes increases. The MAC protocol of the CLIC reduces packet collisions by suppressing packet transmissions that may cause interference and uses a concise reservation channel mechanism to reduce the number of control packets in the network, thus improving network PDR.

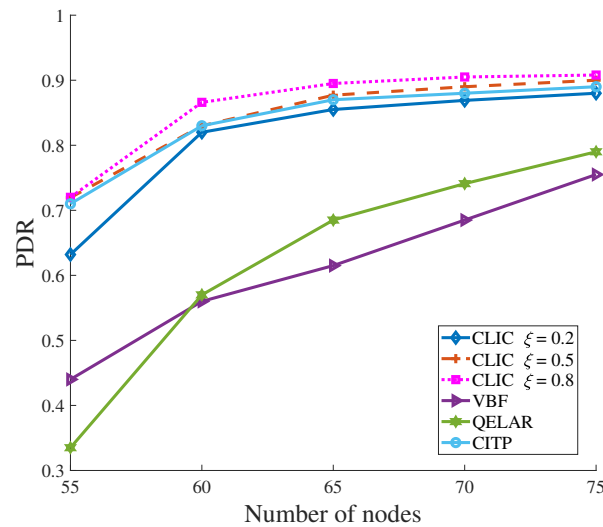


Figure 10. Comparison of PDR versus the number of nodes.

The number of data transmissions in a network has a significant impact on the energy efficiency of the network. For the same number of packets, the higher the number of transmissions, the less energy efficient the network is. As shown in Figure 11, the energy efficient CLIC is higher than that of the QELAR, CITP, and VBF because CLIC integrates

routing-MAC, where the MAC protocol allows packets to be transmitted with minimal overhead, and the routing protocol limits the number of hops to be delivered, thus reducing the number of transmissions. The energy efficiency of CLIC with  $\zeta = 0.8$  is higher than that of  $\zeta = 0.2$ . A low-interference route reduces packet collisions and thus reduces the number of packet transmissions, improving energy efficiency.

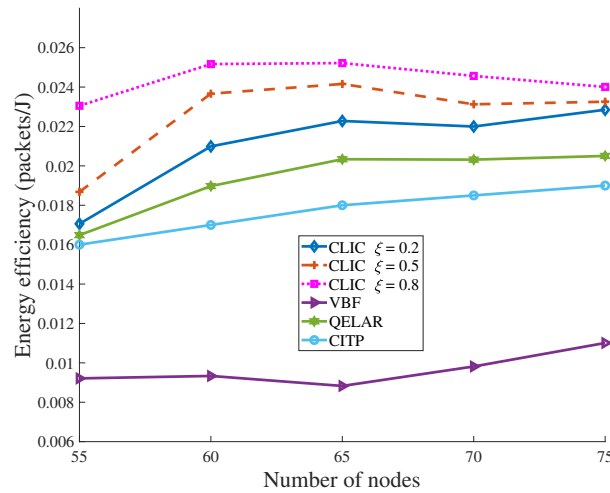


Figure 11. Comparison of energy consumption versus the number of nodes.

Figures 12–14 show a comparison of the performance of protocols at different packet generation rates.

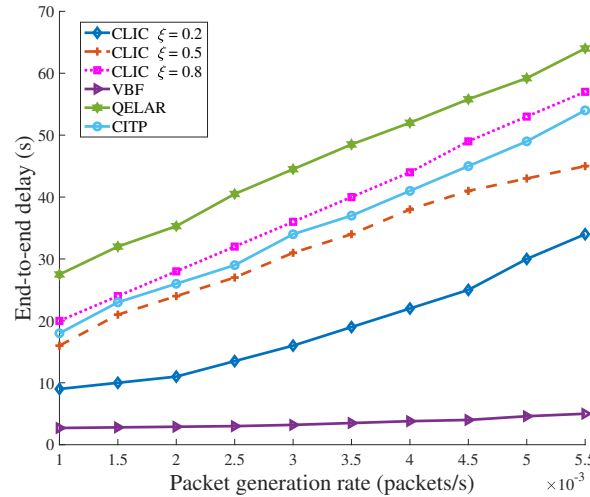


Figure 12. Comparison of end-to-end delay versus packet generation rate.

Figure 12 shows the relationship between the end-to-end delay and packet generation rate of the protocols. The end-to-end delay of CLIC with  $\zeta = 0.2$  is not much higher than that of the VBF, but much less than that of QELAR and CITP. This is because nodes with a high level of congestion have a higher CT priority and can send packets first, thus reducing network congestion and reducing end-to-end delay.

Figure 13 compares the PDR of the protocols under different packet generation rates. The PDR of CLIC and CITP decreases as the packet generation rate increases but is still greater than VBF and QELAR. The increase in packet generation rate leads to an increase in packet collisions. The CITP with  $\zeta = 0.8$  cross-layer takes into account the local interference situation in the network and prevents nodes from transmitting in advance to areas of high interference, thus reducing packet collisions and increasing PDR.

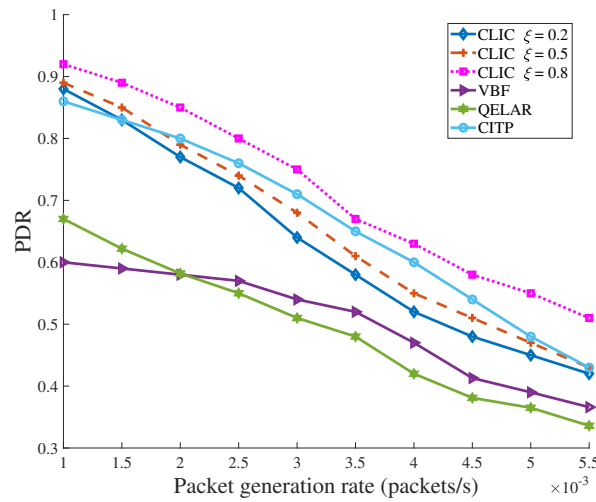


Figure 13. Comparison of PDR versus packet generation rate.

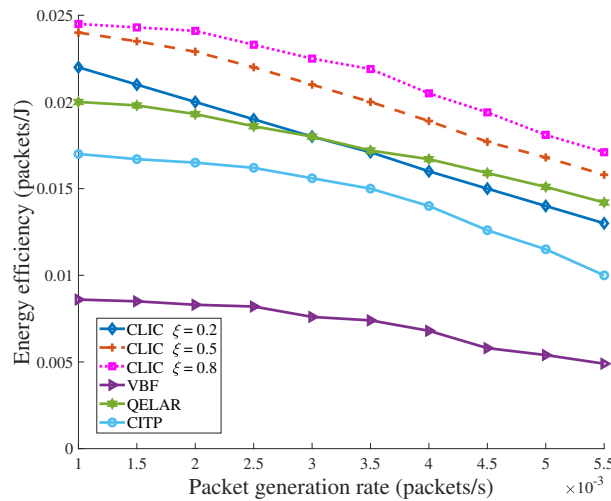


Figure 14. Comparison of energy efficiency versus packet generation rate.

Figure 14 shows the relationship between the energy efficiency and packet generation rate of the protocols. As the packet generation rate increases, there are more packets in the network, leading to an increase in packet collisions. Failed packet transmissions result in more packet transmissions, which lead to a reduction in energy efficiency. Compared with other protocols, CLIC with  $\xi = 0.8$  achieves improvements in energy efficiency because of its focus on network interference.

### 6. Conclusions

The rapid development of acoustic vector sensor technology has led to widespread use of sonar based on vector signal processing in acoustic communication. The directional reception technology can increase spatial reuse and reduce the conflict probability of packets, which is beneficial to improve the performance of UASNs. Therefore, research on underwater sensor network protocols based on directional reception is urgently needed.

In this paper, a cross-layer protocol for low interference and low congestion based on directional reception has been presented and discussed in detail. At the MAC layer, the CLIC uses directional beams to establish data transmission links with minimal interference and maximum capacity. At the routing layer, the CLIC obtains routes with low collision and congestion by weighing the key factors to improve network performance. Simulation results show that the CLIC has higher PDR and higher energy efficiency compared to the QELAR, VBF, and CITP protocols.

The CLIC still has some unresolved routing issues, such as a void region. Due to the limitation of length, we have not addressed the void problem in the manuscript. In future work, we will address this issue.

**Author Contributions:** Y.S. proposed the main ideas, wrote the paper, designed the description framework, conducted the simulations for final approval of the version to be published; W.G. provided guidance for the work and substantial contributions to the analysis; Y.L. reviewed and modified the paper and gave final approval of the version to be published; J.Y. provided guidance for the work and acquired funding and gave final approval of the version to be published. All authors have read and agreed to the published version of the manuscript.

**Funding:** This research was funded by the National Science Foundation for Distinguished Young Scholars of China (Grant No. 62125104).

**Institutional Review Board Statement:** Not applicable.

**Informed Consent Statement:** Not applicable.

**Data Availability Statement:** Not Applicable.

**Acknowledgments:** The authors would like to thank the anonymous reviewers for their time towards the manuscript.

**Conflicts of Interest:** The authors declare no conflict of interest.

## References

- Han, X.; Yin, J.; Tian, Y.; Sheng, X. Underwater acoustic communication to an unmanned underwater vehicle with a compact vector sensor array. *Ocean Eng.* **2019**, *184*, 85–90. [\[CrossRef\]](#)
- Sun, Y.; Zheng, M.; Han, X.; Li, S.; Yin, J. Adaptive clustering routing protocol for underwater sensor networks. *Ad Hoc Netw.* **2022**, *136*, 102953. [\[CrossRef\]](#)
- Yin, J.; Men, W.; Zhu, G.; Han, X. Experimental study of cross-ice acoustic signal propagation. *Appl. Acoust.* **2021**, *172*, 107612. [\[CrossRef\]](#)
- Wang, H.; Huang, Y.; Luo, F.; Yang, L. Multi-Node Joint Power Allocation Algorithm Based on Hierarchical Game Learning in Underwater Acoustic Sensor Networks. *Remote Sens.* **2022**, *14*, 6215. [\[CrossRef\]](#)
- Toor, A.S.; Jain, A. Energy Aware Cluster Based Multi-hop Energy Efficient Routing Protocol using Multiple Mobile Nodes (MEACBM) in Wireless Sensor Networks. *AEU—Int. J. Electron. Commun.* **2019**, *102*, 41–53. [\[CrossRef\]](#)
- Sun, Y.; Zheng, M.; Han, X.; Ge, W.; Yin, J. MOR: Multi-objective routing for underwater acoustic wireless sensor networks. *AEU—Int. J. Electron. Commun.* **2023**, *158*, 154444. [\[CrossRef\]](#)
- Ammar, M.; Ibrahim, K.; Jouhari, M.; Ben-Othman, J. MAC Protocol-Based Depth Adjustment and Splitting Mechanism for Underwater Sensor Network (UWSN). In Proceedings of the 2018 IEEE Global Communications Conference (GLOBECOM), Abu Dhabi, United Arab Emirates, 9–13 December 2018; pp. 1–6. [\[CrossRef\]](#)
- Guan, Z.; Kulhandjian, H.; Melodia, T. Stochastic Channel Access in Underwater Networks with Statistical Interference Modeling. *IEEE Trans. Mob. Comput.* **2021**, *20*, 3020–3033. [\[CrossRef\]](#)
- Liu, Q.; Qiao, G.; Mazhar, S.; Liu, S.; Lou, Y. A Full-Duplex Directional MAC Framework for Underwater Acoustic Sensor Networks. *IEEE Sens. J.* **2022**, *22*, 14647–14661. [\[CrossRef\]](#)
- Yang, J.; Liu, S.; Liu, Q.; Qiao, G. UMDR: Multi-Path Routing Protocol for Underwater Ad Hoc Networks with Directional Antenna. *J. Phys. Conf. Ser.* **2018**, *960*, 012010. [\[CrossRef\]](#)
- Lee, U.; Wang, P.; Noh, Y.; Vieira, L.F.M.; Gerla, M.; Cui, J.H. Pressure Routing for Underwater Sensor Networks. In Proceedings of the 2010 IEEE Infocom, San Diego, CA, USA, 14–19 March 2010; pp. 1–9. [\[CrossRef\]](#)
- Hu, T.; Fei, Y. QELAR: A Machine-Learning-Based Adaptive Routing Protocol for Energy-Efficient and Lifetime-Extended Underwater Sensor Networks. *IEEE Trans. Mob. Comput.* **2010**, *9*, 796–809. [\[CrossRef\]](#)
- Xie, P.; Cui, J.H.; Lao, L. VBF: Vector-Based Forwarding Protocol for Underwater Sensor Networks. In Proceedings of the International Conference on Research in Networking, Lauderdale, FL, USA, 23–25 April 2006.
- Noh, Y.; Lee, U.; Lee, S.; Wang, P.; Vieira, L.F.M.; Cui, J.H.; Gerla, M.; Kim, K. HydroCast: Pressure Routing for Underwater Sensor Networks. *IEEE Trans. Veh. Technol.* **2016**, *65*, 333–347. [\[CrossRef\]](#)
- Yan, H.; Shi, Z.; Cui, J. DBR: Depth-Based Routing for Underwater Sensor Networks. In *Networking 2008 Ad Hoc and Sensor Networks, Wireless Networks, Next Generation Internet*; Springer: Berlin/Heidelberg, Germany, 2008; Volume 4982, pp. 72–86. [\[CrossRef\]](#)
- Wang, K.; Gao, H.; Xu, X.; Jiang, J.; Yue, D. An Energy-Efficient Reliable Data Transmission Scheme for Complex Environmental Monitoring in Underwater Acoustic Sensor Networks. *IEEE Sens. J.* **2016**, *16*, 4051–4062. [\[CrossRef\]](#)

17. Jin, Z.; Zhao, Q.; Su, Y. RCAR: A Reinforcement-Learning-Based Routing Protocol for Congestion-Avoided Underwater Acoustic Sensor Networks. *IEEE Sens. J.* **2019**, *19*, 10881–10891. [[CrossRef](#)]
18. Khan, A.; Ahmedy, I.; Anisi, H.; Javaid, N.; Ihsan, A.; Khan, N.; Alsaqer, M.; Mahmood, H. A Localization-Free Interference and Energy Holes Minimization Routing for Underwater Wireless Sensor Networks. *Sensors* **2018**, *18*, 165. [[CrossRef](#)] [[PubMed](#)]
19. Shashaj, A.; Petroccia, R.; Petrioli, C. Energy efficient interference-aware routing and scheduling in underwater sensor networks. In Proceedings of the 2014 Oceans—St. John’s, St. John’s, NL, Canada, 14–19 September 2014; pp. 1–8. [[CrossRef](#)]
20. Zhao, R.; Li, N.; Dobre, O.A.; Shen, X. CITP: Collision and Interruption Tolerant Protocol for Underwater Acoustic Sensor Networks. *IEEE Commun. Lett.* **2020**, *24*, 1328–1332. [[CrossRef](#)]
21. Bharamagoudra, M.R.; Manvi, S.S.; Gonen, B. Event driven energy depth and channel aware routing for underwater acoustic sensor networks: Agent oriented clustering based approach. *Comput. Electr. Eng.* **2017**, *58*, 1–19. [[CrossRef](#)]
22. Li, J.; Wang, J.; Wang, X.; Qiao, G.; Luo, H.; Gulliver, T.A. Optimal Beamforming Design for Underwater Acoustic Communication With Multiple Unsteady Sub-Gaussian Interferers. *IEEE Trans. Veh. Technol.* **2019**, *68*, 12381–12386. [[CrossRef](#)]
23. Yang, T.C. Deconvolved Conventional Beamforming for a Horizontal Line Array. *IEEE J. Ocean. Eng.* **2018**, *43*, 160–172. [[CrossRef](#)]
24. Poursheikhali, S.; Zamiri-Jafarian, H. Received signal strength based localization in inhomogeneous underwater medium. *Signal Process.* **2019**, *154*, 45–56. [[CrossRef](#)]
25. Hou, X.; Qiao, Y.; Zhang, B.; Yang, Y. Robust Underwater Direction-of-Arrival Tracking Based on AI-Aided Variational Bayesian Extended Kalman Filter. *Remote Sens.* **2023**, *15*, 420. [[CrossRef](#)]
26. Liu, F.; Tian, L.a.; Liu, K.; Wang, G. Matched-field localization with single vector hydrophone in shallow water. In Proceedings of the 2017 IEEE International Conference on Signal Processing, Communications and Computing (ICSPCC), Xiamen, China, 22–25 October 2017; pp. 1–5. [[CrossRef](#)]

**Disclaimer/Publisher’s Note:** The statements, opinions and data contained in all publications are solely those of the individual author(s) and contributor(s) and not of MDPI and/or the editor(s). MDPI and/or the editor(s) disclaim responsibility for any injury to people or property resulting from any ideas, methods, instructions or products referred to in the content.